

Unraveling Hidden Infrared Spectral Signatures in PFAS Thermal Degradation with Two-Dimensional Correlation Spectroscopy

Nicholas Stavinski, Runze Sun, Alireza Arhami Dolatabad, Mohamed Ateia,* Feng Xiao,* and Luis Velarde*



Cite This: <https://doi.org/10.1021/acs.estlett.5c00192>



Read Online

ACCESS |

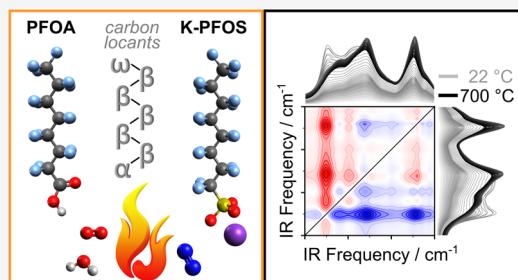
Metrics & More

Article Recommendations

Supporting Information

ABSTRACT: Per- and polyfluoroalkyl substances (PFAS) are difficult to degrade into more innocuous chemical species, which makes investigating their molecular characteristics at increased temperatures crucial for effective thermal PFAS remediation strategies. This Letter reports on the first development and implementation of infrared (IR) two-dimensional correlation spectroscopy (2D-COS) to elucidate hidden vibrational modes of gas-phase perfluoroctanoic acid (PFOA, $C_8F_{15}O_2H$) and the potassium salt of perfluoroctanesulfonic acid (K-PFOS, $C_8F_{17}SO_3HK$) undergoing thermal degradation (22–700 °C) in both N_2 and air environments. Carbon–fluorine moieties unnoticed in conventional one-dimensional (1D) IR spectra were revealed via 2D-COS. Their spectral features were cross-correlated with other observed PFAS vibrations to distinguish peaks originating from the initial parent molecule and those of the degradation byproducts. Rotational–vibrational (rovibrational) spectra were observed for K-PFOS in air, a result that may be leveraged to extract fundamental structural properties of gas-phase PFAS. Overall, we observed distinct carbon–fluorine vibrational modes in PFOA and K-PFOS, providing unique mechanistic insights, such as bond scission at different carbon locants. The methodology and findings reported herein are critical to illustrating how different molecular configurations affect degradation pathways, offering a deeper understanding of PFAS behavior under thermal conditions.

KEYWORDS: PFAS, products of incomplete destruction, thermal degradation, 2D-COS, IR spectroscopy



1. INTRODUCTION

Per- and polyfluoroalkyl substances (PFAS) have been extensively detected in environmental matrices, including natural waters, wastewaters, soils, biosolids, and landfill leachates.^{1–11} Recent regulations by the U.S. Environmental Protection Agency have listed several PFAS, including perfluoroctanoic acid (PFOA) and perfluoroctanesulfonic acid (PFOS), as hazardous substances under the Comprehensive Environmental Response, Compensation, and Liability Act¹² and the Safe Drinking Water Act,¹³ highlighting the urgent need for remediation technologies. Several thermal-based techniques have been explored for treating PFAS-laden spent media from water treatment facilities, as well as a variety of contaminated materials, including soil, biosolids, and municipal solid waste.^{14–21} While these techniques (e.g., incineration,^{22–25} pyrolysis,^{26–29} smoldering,^{30,31} thermal desorption,^{32–34} and dry air oxidation^{17,18,35}) have shown promising results in the laboratory, and even full-scale applications, multiple studies have reported that incomplete destruction of PFAS can generate byproducts,^{17,32,35–41} including fluorinated greenhouse gases. Therefore, studies on products of incomplete destruction (PIPs) of PFAS are essential to understanding and mitigating the environmental impacts associated with these thermal treatment processes.

Various methodologies have been developed to detect and quantify PIPs of PFAS (Table S1). Techniques such as liquid chromatography–mass spectrometry are valued for their sensitivity in quantitative analysis,^{42–44} although they require complex sample preparation that may alter the chemical integrity of samples. Gas chromatography–mass spectrometry, while offering high sensitivity and specificity for volatile, semivolatile, and neutral PFAS,^{45–47} is limited by the thermal stability of these compounds, necessitating extensive pretreatment that can compromise the accuracy of detection. Fourier-transform infrared (FTIR) spectroscopy provides an alternative approach with comparable sensitivity to mass spectrometry. FTIR spectroscopy relies on a reference library for the identification and quantification of specific PFAS,^{48–50} which limits detection to the number of available standards but allows for more precise results.

Received: February 26, 2025

Revised: March 31, 2025

Accepted: April 1, 2025

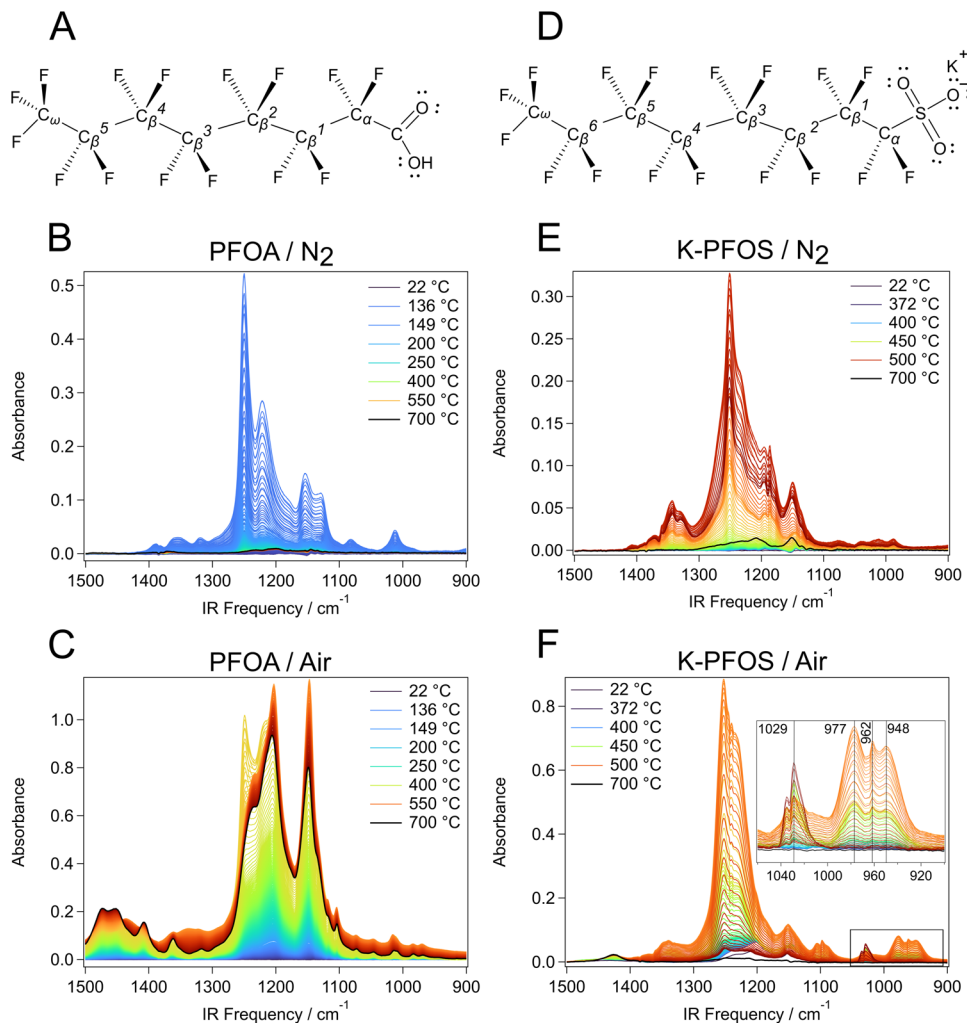


Figure 1. Molecular structures of (A) perfluorooctanoic acid (PFOA, C₈F₁₅OOH) and (D) potassium perfluoroctanesulfonate (K-PFOS, C₈F₁₇SO₃HK). Dynamic 1D-FTIR spectra of PFOA being heated in (B) N₂ and (C) air. Dynamic 1D-FTIR spectra of K-PFOS being heated from 22 to 700 °C in (E) N₂ and (F) air.

Recently, FTIR coupled with thermogravimetric analysis (TGA-FTIR)^{41,51,52} has been used to provide real-time analysis of gases evolving from the TGA furnace, enabling direct measurement without complex sample preparation. However, analyzing dynamic spectral data sets poses challenges due to the subtlety of inter- and intramolecular interactions.⁵² In this study, we utilize state-of-the-art methods that enhance the spectral resolution of gas-phase PFAS FTIR spectra. We demonstrate that two-dimensional correlation spectroscopy (2D-COS)^{53,54} can reveal hidden details in PFAS PIDs. This advancement is critical for understanding the complex behavior of PFAS. By uncovering previously undetectable degradation pathways and molecular interactions, our approach provides a tool to inform the development of targeted remediation strategies, ultimately advancing efforts to mitigate the environmental and health impacts of these pervasive pollutants. To the best of our knowledge, this is the first study applying 2D-COS to PFAS FTIR spectra, revealing molecular interactions and degradation mechanisms previously undetectable through 1D-FTIR analysis.

2. METHODS AND MATERIALS

Perfluorooctanoic acid (PFOA, 95%) and the potassium salt of perfluorooctanesulfonic acid (K-PFOS, ≥98.0%) were procured from Sigma-Aldrich. The PFOA and K-PFOS powders were dried at 40 °C to remove residual moisture, enhancing their reactivity for thermal analyses. The samples were ground into a fine powder to maximize surface exposure, increasing the efficacy and consistency of the thermal degradation processes. TGA-FTIR analysis was performed using a Thermal Analysis Laboratory at Western Kentucky University. Samples (5.4–12.5 mg) were placed in a ceramic cup and distributed evenly to prevent uneven heating or hot spots. The samples underwent thermal analysis using a model TA Q600 SDT TGA instrument connected to a PerkinElmer Spectrum ONE FTIR instrument via a heated stainless-steel transfer line and gas cell. This setup maintained the samples isothermally at room temperature for 30 min before heating to 700 or 800 °C at a rate of 10 °C/min, under a controlled atmosphere of air or nitrogen (N₂) flowing at a rate of 100 mL/min. The evolving gases were channeled through the transfer line into an IR gas cell equipped with KBr windows and kept at 150 °C to prevent condensation. The path length of the FTIR cell is 2 ft. Spectra of 2 cm⁻¹ resolution were recorded from 700 to 4000 cm⁻¹.

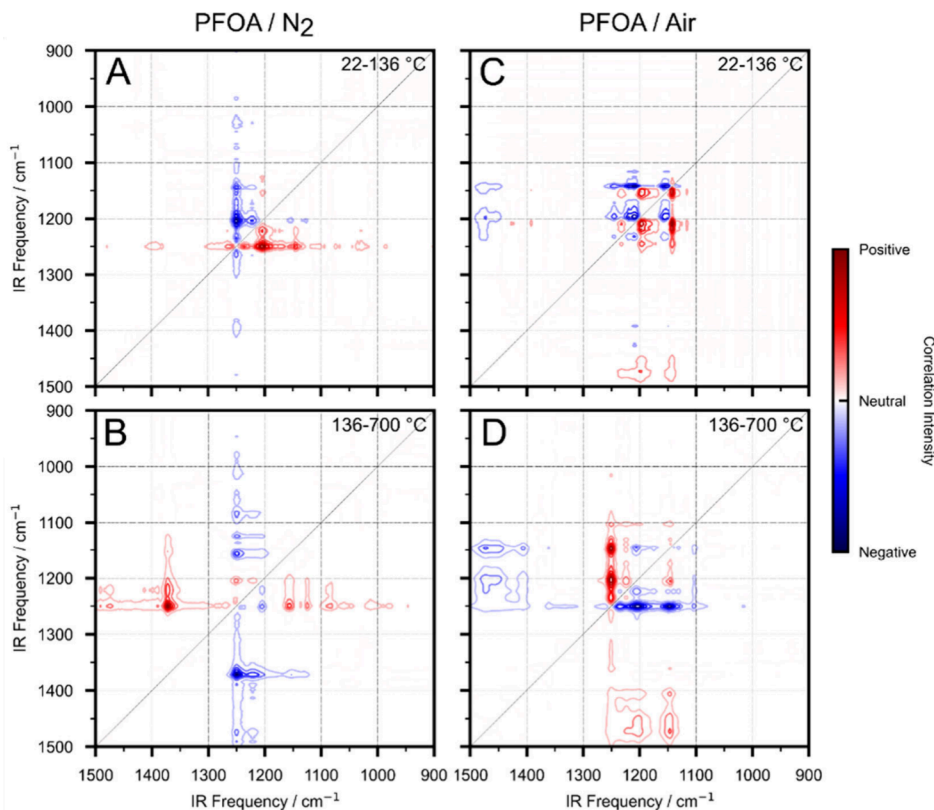


Figure 2. 2D-COS asynchronous spectra of PFOA in (A) 22–136 and (B) 136–700 °C. Asynchronous spectra of PFOA in air at (C) 22–136 and (D) 136–700 °C.

using relatively large sample quantities to ensure the detection of “trace-level” PIDs. 2D-COS plots were generated using the 2Dpy package developed by Morita (Supporting Information).^{55–58}

3. RESULTS AND DISCUSSION

3.1. Analysis of Carbon–Fluorine (C–F) Moieties and Rotation–Vibration Spectra. The vibrational characteristics of PFOA and K-PFOS, two benchmark⁵⁹ compounds with unique properties, were examined side by side to provide complementary insights about their dynamic behavior under thermal conditions. The C atom locants (α , β , and ω) depicted in panels A and D of Figure 1 help specify the C–F moieties in Tables S2–S5. The wavenumber range of 900–1500 cm^{−1} was chosen because it spans most of the “molecular fingerprint region”. However, there are numerous C–F vibrational modes that overlap in 1D-FTIR spectra. Figure 1A highlights the notation that can be used to label several important PFOA vibrations, such as $\nu_{as}(C_1^1–F_2)$, $\nu_{as}(C_\omega F_3)$, $\nu(C_\omega–C_\beta^1)$, and $\nu_{as}(C_\beta^1 C_\beta^2 C_\beta^3)$, corresponding to chain stretching modes that are either symmetric or antisymmetric (as).⁶⁰ Their spectral signatures are central for understanding molecular-level mechanisms involving bond scission, inter- and intramolecular interactions, the degree of bond substitution, and isomer formation.^{17,35}

During thermal degradation, PFAS of different chain lengths may form simultaneously, leading to increased spectral congestion. For example, the IR bands of perfluoroheptane (C_7F_{16}) at 1100–1400 cm^{−1} have been shown⁶¹ to increase by 3–7 cm^{−1} when expanding the chain length by one C atom (perfluorooctane, C_8F_{18}). However, some vibrational frequencies may shift to lower frequencies, or even remain unchanged,

with an increase in chain length. Identifying these nuances is crucial for advancing the field of PFAS processing.

Figure 1 presents the dynamic 1D-FTIR spectra of PFOA (Figure 1B,C) and K-PFOS (Figure 1E,F) at 22–700 °C. The PFOA and K-PFOS IR band intensities achieve maximum absorbance at 136 and 500 °C, respectively, as the molecules enter the gas phase.¹⁴ Since intensities reflect the mode oscillator strength and number density of an IR-active functional group, the absorbance of a band in these experiments reflects on the abundance of gas-phase species. For example, Figure 1B shows minimal evidence of the remaining PFOA and degradation species at 700 °C. Figure 1C, PFOA in air, suggests otherwise, as oxidation likely plays a key role in the formation and persistence of molecular degradation products at >700 °C.

The IR frequency of the antisymmetric modes reported herein agreed with recent computations^{62–64} (Tables S2–S5). Reported IR vibration assignments are curated in Tables S2–S5. In Figure 1F, two broad bands at 948 and 977 cm^{−1} resembling the *P*- and *R*-branches, respectively, of the carbonyl rovibrational spectrum of COF₂⁶⁵ were observed. These bands arise because vibrational transitions in the gas phase are accompanied by rotational transitions.⁶⁶ At their center (~962 cm^{−1}), a sharp and intense band corresponding to the *Q*-branch is resolved. The presence of a collective *P*, *Q*, and *R*-branch triad suggests the dipole moment of this particular vibration (e.g., carbonyl bend) oscillates perpendicular to the molecular axis. Additionally, the band at 1029 cm^{−1} at ~600 °C could be assigned to either a *Q*-branch of an anhydride bend or a parallel band of a sulfoxide stretch. In the case of a parallel band, where the dipole moment oscillates parallel to the molecular axis, only a *P*-branch and an *R*-branch would be

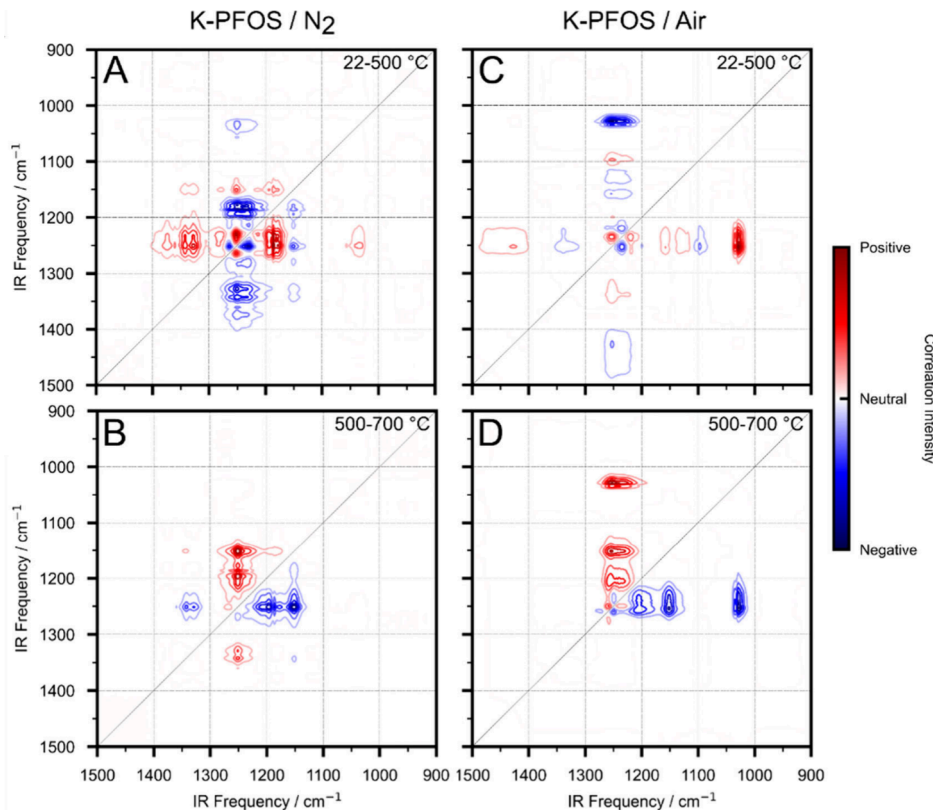


Figure 3. Asynchronous spectra of K-PFOS in N_2 at (A) 22–500 and (B) 500–700 °C. Asynchronous spectra of K-PFOS in air at (C) 22–500 and (D) 500–700 °C.

expected with no sharp Q-branch.⁶⁶ These observations are key because higher-resolution rovibrational spectra may be used in future studies to determine structural properties of PFAS and their degradation products.

3.2. Enhanced Spectral Resolution via 2D-COS of PFOA. A 2D-COS procedure was applied to the dynamic 1D-FTIR spectra of gas-phase PFOA and K-PFOS undergoing thermal degradation. Synchronous 2D spectra reflect simultaneous changes in signal over an external perturbation. Asynchronous 2D spectra may reveal vibrational modes that change out of phase or modes that were otherwise hidden in the 1D spectra (Tables S2–S5). The enhanced spectral resolution achieved using 2D-COS may provide new insights about molecular-level phenomena that can be leveraged for the mitigation of hazardous PFAS degradation pathways.

Figure 2 presents the asynchronous spectra of PFOA thermal degradation in an inert N_2 atmosphere (Figure 2A,B) and in air (Figure 2C,D). The analysis was performed by separating the data sets such that the 22–136 °C data set represents increasing absorbance (minimum to maximum) and the 136–700 °C data set represents decreasing absorbance (maximum to minimum), as shown in panels B, C, E, and F of Figure 1. Therefore, the 2D bands reflect the absorbance intensity change of PFAS vibrations during the liquid- to gas-phase transition, and the subsequent entry of the molecules into the instrument's IR beam path. For example, the combination band, $\nu_{\text{as}}(\text{CF}_2) + \nu_{\text{as}}(\text{CF}_3)$, at 1204 cm^{-1} is observed in Figure 2A but absent in the corresponding 1D analogue (Figure 1B). The PFOA $\text{C}_\alpha\text{F}_2$, C_βF_2 , and $\text{C}_\omega\text{F}_3$ vibrational modes have recently been calculated using density functional theory, with the latter two considered to be the most challenging to defluorinate.^{62,67}

Cross-peaks in Figure 2A show positive correlation between the C_βF_2 stretching modes at 1075, 1104, 1115, 1125, and 1145 cm^{-1} and the most intense $\nu_{\text{as}}(\text{CF}_2)$ band at 1250 cm^{-1} , which indicates the appearance of the gas-phase C_βF_2 modes during the phase transition at 22–136 °C (Figure 2A). At 136–700 °C, these C_βF_2 correlation peaks disappear (Figure 2B). This observation is important because the $\nu(\text{C}_\beta\text{F}_2)$ and $\nu_{\text{as}}(\text{C}_\beta^{4-1}\text{F}_2)$ modes are not observed for PFOA under N_2 in the 1D spectra (Figure 1B and Table S2).

When PFOA was thermally degraded under air at 22–136 °C, the $\nu(\text{C}_\beta^5\text{F}_2)$ and $\nu_{\text{as}}(\text{C}_\beta^{4-1}\text{F}_2)$ cross-correlation peaks with the 1250 cm^{-1} mode were observed at 1130 and 1142 cm^{-1} , respectively, which are a few wavenumbers shifted to higher and lower IR frequencies compared to the corresponding experimental bands of PFOA in N_2 . The C–F bond stretching modes are sensitive to electrostatic interactions, exhibiting a vibrational Stark effect.⁶⁸ Therefore, vibrational frequency shifts may be attributed to conformational effects or varying degrees of hydrogen bonding (HB) interactions with water vapor inside the thermal chamber. The prediction of HB in fluorine systems is an ongoing research topic.^{69,70} For instance, Pietruš et al. presented a study on monofluoroanilines in which a decrease in IR frequency for N–H vibrations in the presence of fluorine atoms was observed.⁷¹ Comparing Tables S2 and S3 for C–F vibrations that may be susceptible to HB, it is possible that varying stabilities of these interactions lead to shifted IR frequencies of the C_βF_2 modes.

Evidence of the removal of the carboxylic acid “head” group, -COOH, may be determined by inspection of the $\nu(\text{C}_\alpha-\text{C}_{\text{acid}})$ mode, calculated to occur at 1316 cm^{-1} by Jenness et al.⁶² An IR band at 1298 cm^{-1} may be tentatively assigned to this vibration under N_2 , but further study is needed, as this

vibration is likely weak in intensity and prone to frequency shifting, especially under air with possible dimer formation. Evidence of the $\nu(C_\alpha F_2)$ stretch at 1060–66 cm^{-1} was observed, but only under N_2 (Figure 2B). With regard to the end group or “tail” $\delta(C_\omega F_3)$, the breathing mode and antisymmetric stretch were observed under air and N_2 (Tables S2 and S3). Examining how HB impacts the vibrational frequencies of C–F moieties at different carbon locants may help elucidate degradation processes such as chain scission.

3.3. Enhanced Spectral Resolution via 2D-COS of K-PFOS. Figure 3 presents the asynchronous spectra of K-PFOS undergoing thermal degradation. Temperature ranges of 22–500 and 500–700 $^\circ\text{C}$ were chosen to align with recent reports^{72–74} investigating thermal-phase transitions in addition to the explanation of the methods in section 3.1. Specifically, the phase change is captured in panels A and C of Figure 3 for N_2 and air conditions, respectively. The $\nu(C_\beta F_2)$, $\rho(C_\beta^{6-3})$, $\nu(C_\beta^2-C_\beta^3)$, and $\nu_{as}(C_\omega F_3)$ modes are not shown in Figure 3A but are present in Figure 3C, suggesting that the dichotomy of environmental conditions inside thermal chambers may be leveraged for studying the fundamental vibrations.

Vibrations corresponding to sulfonic acid, such as $\nu_{as}(C_\beta^1 C_\alpha C_{acid})$ at 1186 cm^{-1} , $\nu_{as}(\text{R}-\text{SO}_3^-)$ at 1218 cm^{-1} , and the sulfoxide stretch at 1338 cm^{-1} , vanished under air at >500 $^\circ\text{C}$ (Table S5), implying this acid group is removed from the parent chain. Interestingly, while the band at ~ 1250 –1253 cm^{-1} remained present in both environmental conditions at >500 $^\circ\text{C}$, under N_2 , the correlation intensity changes from positive (red) to negative (blue); this is indicative of the predicted $\nu_{as}(\text{CF}_2) + \nu_{as}(\text{R}-\text{SO}_3^-)$ combination band assignment in K-PFOS, as it would be expected to appear after the phase change and then disappear with respect to the perturbation variable since degradation occurs. On the contrary, in air, the correlation intensity stays positive, meaning the 1253 cm^{-1} peak in Figure 3D and Table S5 likely originates from a byproduct.

3.4. Heteromode and Heteroperturbation 2D-COS Analysis. Heterocorrelation 2D-COS may be implemented into novel control technologies such as autonomous sensing devices for PFAS emissions. To demonstrate this utility on the proof-of-concept sample systems of PFOA and K-PFOS, Figure 4 presents a heterocorrelation analysis on different IR regions (e.g., heteromode (Figure 4A)) and different thermal environment perturbations (e.g., heteroperturbation (Figure 4B)). This technique, when applied with different spectral probes and perturbations, may assist with the validation of PIDs and other PFAS.

Inapparent IR bands of the thermal decomposition products of carbonyl fluoride (COF_2) and silicon tetrafluoride (SiF_4) were validated using a heteromode and heteroperturbation analysis (Figure 4). Figure 4A presents the characteristic COF_2 bands⁷⁵ at 950–1000 and 1880–1980 cm^{-1} . A weak IR band is expected to be centered at 850 cm^{-1} , and it was subtly elucidated via synchronous 2D-COS and positively correlated with the P -, Q -, and R -branches at 1935–1950 cm^{-1} (Figure S6). By relying on strong, distinctive IR signals, such as those at 1935–1950 cm^{-1} , heteroprobe analysis enables a pairwise comparison that may enable the assignment of weaker vibrational modes that have gone unreported. In other words, knowledge from well-characterized spectral regions may be extended to regions that are less understood.

Figure 4B presents an asynchronous heteroperturbation correlation spectrum in which two different data sets, K-PFOS

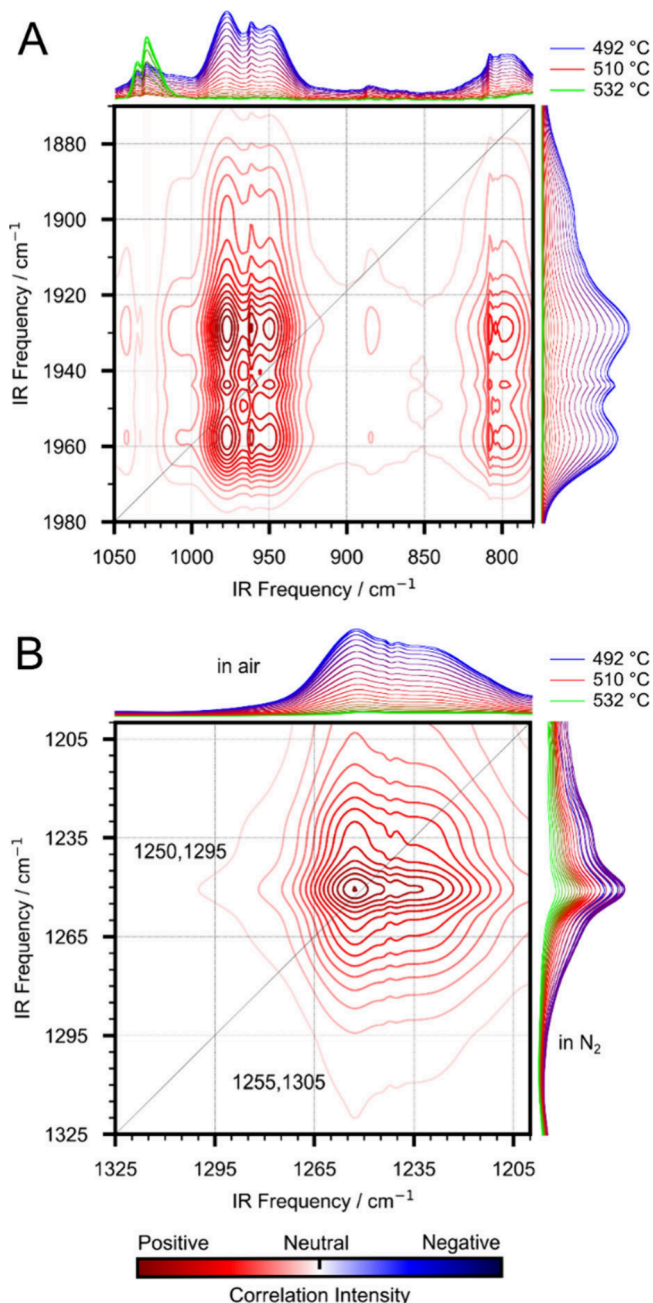


Figure 4. (A) Heteromode synchronous spectrum of K-PFOS in air at 492–532 $^\circ\text{C}$ for 780–1050 and 1870–1980 cm^{-1} . (B) Heteroperturbation asynchronous spectrum of K-PFOS in air and N_2 at 492–532 $^\circ\text{C}$ for 1200–1325 cm^{-1} . Asymmetry at the x , y coordinates of 1250, 1295 cm^{-1} and 1255, 1305 cm^{-1} , respectively, validate the formation of SiF_4 and COF_2 from K-PFOS in air.

in air and K-PFOS in N_2 at 1200–1325 cm^{-1} , are correlated. Figure 4B resolves a weak IR band⁷⁶ at 1300 cm^{-1} that originates from SiF_4 . Additionally, by referring to the diagonal line in Figure 4B, an asymmetry in the overall 2D plot is observed. This suggests a difference in the rate of change for the IR-active vibrational modes present in the system. For the N_2 environment, where SiF_4 is unobserved, the band at around 1250 cm^{-1} may correspond to $\nu_{as}(\text{CF}_2) + \nu_{as}(\text{R}-\text{SO}_3^-)$, suggesting the higher IR frequency reported in Table S5 may correspond to COF_2 and not necessarily the parent molecule, K-PFOS.⁷⁵ This result further highlights the role that oxygen

plays in generating SiF₄ and COF₂. Future 2D-COS experiments may help differentiate PFAS from PIDs (Tables S2–S5). Heteroperturbation 2D-COS may help elucidate how the vibrational frequencies of PFAS moieties respond to different environments, thus establishing a basis for practical implementation of this technique.

4. ENVIRONMENTAL IMPLICATIONS

This study expands the existing tool kit for understanding PFAS degradation by leveraging two-dimensional spectroscopy. Analyses revealed distinct vibrational behaviors of C–F bonds in PFOA and K-PFOS within the “molecular fingerprint region”, demonstrating how varying chain lengths and thermal conditions influence both the frequency and the intensity of IR bands. This offers important clues about degradation pathways. The ability of 2D-COS to uncover hidden vibrational modes and resolve subtle frequency shifts offers deeper insight into the molecular interactions and transformations during PFAS thermal degradation.

A key finding of our research is the identification of inter- and intramolecular interactions that occur during thermal stress processing. For instance, hydrogen bonding in the C_βF₂ and C_ωF₃ moieties provides molecular-level insights into how thermal conditions promote bond scission. This information is essential for predicting the behavior of PFAS in real-world environments where thermal degradation may occur under varied conditions, such as incineration or high-temperature industrial processing. Moreover, our findings highlight the potential of 2D-COS to serve as a predictive tool in environmental remediation strategies.

■ ASSOCIATED CONTENT

SI Supporting Information

The Supporting Information is available free of charge at <https://pubs.acs.org/doi/10.1021/acs.estlett.5c00192>.

Additional information regarding the methodology, data, and results ([PDF](#))

■ AUTHOR INFORMATION

Corresponding Authors

Mohamed Ateia — *Center for Environmental Solutions & Emergency Response, U.S. Environmental Protection Agency, Cincinnati, Ohio 45268, United States; Department of Chemical and Biomolecular Engineering, Rice University, Houston, Texas 77005-1827, United States;* [orcid.org/0000-0002-3524-5513](#); Email: mohamedateia1@gmail.com

Feng Xiao — *Department of Civil and Environmental Engineering, University of Missouri, Columbia, Missouri 65211, United States; Missouri Water Center, University of Missouri, Columbia, Missouri 65211, United States;* [orcid.org/0000-0001-5686-6055](#); Email: Feng.Xiao@missouri.edu

Luis Velarde — *Department of Chemistry, University at Buffalo, State University of New York (SUNY), Buffalo, New York 14260, United States;* [orcid.org/0000-0001-6329-3486](#); Email: lvelarde@buffalo.edu

Authors

Nicholas Stavinski — *Department of Chemistry, University at Buffalo, State University of New York (SUNY), Buffalo, New*

York 14260, United States; [orcid.org/0000-0002-6567-1409](#)

Runze Sun — *Department of Civil and Environmental Engineering, University of Missouri, Columbia, Missouri 65211, United States*

Alireza Arhami Dolatabad — *Department of Civil and Environmental Engineering, University of Missouri, Columbia, Missouri 65211, United States;* [orcid.org/0000-0002-8740-0757](#)

Complete contact information is available at:
<https://pubs.acs.org/10.1021/acs.estlett.5c00192>

Notes

The views expressed in this article are those of the author(s) and do not necessarily represent the views or the policies of the U.S. Environmental Protection Agency (EPA). The research presented was not performed or funded by EPA and was not subject to EPA's quality system requirements. This document has been subjected to the EPA's review and has been approved for publication.

The authors declare no competing financial interest.

■ ACKNOWLEDGMENTS

Manuscript development was supported by the U.S. Department of Defense SERDP (ER22-4014), the Environmental Research & Education Foundation, and the U.S. National Science Foundation CAREER Program (Grants 2320966 and 1753207).

■ REFERENCES

- (1) Zhou, T.; Li, X.; Liu, H.; Dong, S.; Zhang, Z.; Wang, Z.; Li, J.; Nghiem, L. D.; Khan, S. J.; Wang, Q. Occurrence, fate, and remediation for per- and polyfluoroalkyl substances (PFAS) in sewage sludge: A comprehensive review. *J. Hazard Mater.* **2024**, *466*, 133637.
- (2) Moavenzadeh Ghaznavi, S.; Zimmerman, C.; Shea, M. E.; MacRae, J. D.; Peckenham, J. M.; Noblet, C. L.; Apul, O. G.; Kopce, A. D. Management of per- and polyfluoroalkyl substances (PFAS)-laden wastewater sludge in Maine: Perspectives on a wicked problem. *Biointerphases* **2023**, *18* (4), 041004.
- (3) Wanzek, T. A.; Field, J. A.; Kostarelos, K. Repeated Aqueous Film-Forming Foams Applications: Impacts on Polyfluoroalkyl Substances Retention in Saturated Soil. *Environ. Sci. Technol.* **2024**, *58* (3), 1659–1668.
- (4) Davis, M. J. B.; Evich, M. G.; Goodrow, S. M.; Washington, J. W. Environmental Fate of Cl-PFPECA: Accumulation of Novel and Legacy Perfluoroalkyl Compounds in Real-World Vegetation and Subsoils. *Environ. Sci. Technol.* **2023**, *57* (24), 8994–9004.
- (5) Xiao, F.; Simcik, M. F.; Halbach, T. R.; Gulliver, J. S. Perfluorooctane sulfonate (PFOS) and perfluorooctanoate (PFOA) in soils and groundwater of a U.S. metropolitan area: Migration and implications for human exposure. *Water Res.* **2015**, *72*, 64–74.
- (6) Xiao, F.; Halbach, T. R.; Simcik, M. F.; Gulliver, J. S. Input characterization of perfluoroalkyl substances in wastewater treatment plants: Source discrimination by exploratory data analysis. *Water Res.* **2012**, *46* (9), 3101–3109.
- (7) Islam, M.; Thompson, K.; Dickenson, E.; Quiñones, O.; Steinle-Darling, E.; Westerhoff, P. Sucralose and Predicted De Facto Wastewater Reuse Levels Correlate with PFAS Levels in Surface Waters. *Environ. Sci. Technol. Lett.* **2023**, *10* (5), 431–438.
- (8) Houtz, E. F.; Sutton, R.; Park, J. S.; Sedlak, M. Poly- and perfluoroalkyl substances in wastewater: Significance of unknown precursors, manufacturing shifts, and likely AFFF impacts. *Water Res.* **2016**, *95*, 142–149.
- (9) Song, D.; Qiao, B.; Yao, Y.; Zhao, L.; Wang, X.; Chen, H.; Zhu, L.; Sun, H. Target and nontarget analysis of per- and polyfluoroalkyl

- substances in surface water, groundwater and sediments of three typical fluorochemical industrial parks in China. *J. Hazard Mater.* **2023**, *460*, 132411.
- (10) Wang, Q.; Ruan, Y. F.; Yuen, C. N. T.; Lin, H. J.; Yeung, L. W. Y.; Leung, K. M. Y.; Lam, P. K. S. Tracing per- and polyfluoroalkyl substances (PFASs) in the aquatic environment: Target analysis and beyond. *Trac-Trend Anal Chem.* **2023**, *169*, 117351.
- (11) Wang, T.; Vestergren, R.; Herzke, D.; Yu, J.; Cousins, I. T. Levels, isomer profiles, and estimated riverine mass discharges of perfluoroalkyl acids and fluorinated alternatives at the mouths of Chinese rivers. *Environ. Sci. Technol.* **2016**, *50* (21), 11584–11592.
- (12) U.S. EPA. Designation of PFOA and PFOS as hazardous substances under CERCLA Release Reporting Requirements Fact sheet. 2024. <https://www.epa.gov/epcra/designation-pfoa-and-pfoss-hazardous-substances-under-cercla-release-reporting-requirements> (accessed April 2024).
- (13) U.S. EPA. Final PFAS National Primary Drinking Water Regulation. 2024. <https://www.epa.gov/sdwa/and-polyfluoroalkyl-substances-pfas> (accessed April 2024).
- (14) Xiao, F.; Challa Sasi, P.; Alinezhad, A.; Sun, R.; Abdulmalik Ali, M. Thermal Phase Transition and Rapid Degradation of Forever Chemicals (PFAS) in Spent Media Using Induction Heating. *ACS ES&T Eng.* **2023**, *3* (9), 1370–1380.
- (15) Wang, Z.; Alinezhad, A.; Sun, R.; Xiao, F.; Pignatello, J. J. Pre- and Postapplication Thermal Treatment Strategies for Sorption Enhancement and Reactivation of Biochars for Removal of Per- and Polyfluoroalkyl Substances from Water. *ACS ES&T Engineering* **2023**, *3* (2), 193–200.
- (16) Sun, R. Z.; Sasi, P. C.; Alinezhad, A.; Xiao, F. Sorptive removal of per- and polyfluoroalkyl substances (PFAS) in organic-free water, surface water, and landfill leachate and thermal reactivation of spent sorbents. *J. Hazard Mater. Adv.* **2023**, *10*, 100311.
- (17) Alinezhad, A.; Shao, H.; Litvanova, K.; Sun, R. Z.; Kubatova, A.; Zhang, W.; Li, Y.; Xiao, F. Mechanistic Investigations of Thermal Decomposition of Perfluoroalkyl Ether Carboxylic Acids and Short-Chain Perfluoroalkyl Carboxylic Acids. *Environ. Sci. Technol.* **2023**, *57* (23), 8796–8807.
- (18) Sasi, P. C.; Alinezhad, A.; Yao, B.; Kubatova, A.; Golovko, S. A.; Golovko, M. Y.; Xiao, F. Effect of granular activated carbon and other porous materials on thermal decomposition of per- and polyfluoroalkyl substances: Mechanisms and implications for water purification. *Water Res.* **2021**, *200*, 117271.
- (19) Xiao, F.; Sasi, P. C.; Yao, B.; Kubatova, A.; Golovko, S. A.; Golovko, M. Y.; Soli, D. Thermal stability and decomposition of perfluoroalkyl substances on spent granular activated carbon. *Environ. Sci. Technol. Lett.* **2020**, *7* (5), 343–350.
- (20) Soker, O.; Hao, S. L.; Trewyn, B. G.; Higgins, C. P.; Strathmann, T. J. Application of Hydrothermal Alkaline Treatment to Spent Granular Activated Carbon: Destruction of Adsorbed PFASs and Adsorbent Regeneration. *Environ. Sci. Technol. Lett.* **2023**, *10* (5), 425–430.
- (21) Zhang, Q.; Mian, M. M.; Zhang, A.; Zhou, L.; Du, R.; Ao, W.; Yu, G.; Deng, S. Catalytic Degradation of Hexafluoropropylene Oxide Trimeric Acid during the Hydrothermal Regeneration of Spent Activated Carbon. *ACS ES&T Engineering* **2024**, *4* (6), 1391–1400.
- (22) Cornell, R. E.; Burke, M. P. Low-temperature oxidation pathways are critical to thermal incineration of PFAS-laden materials. *J. Hazard Mater. Lett.* **2024**, *5*, 100100.
- (23) Blotevogel, J.; Giraud, R. J.; Rappé, A. K. Incinerability of PFOA and HFPO-DA: Mechanisms, kinetics, and thermal stability ranking. *Chemical Engineering Journal* **2023**, *457*, 141235.
- (24) Altarawneh, M.; Almatarneh, M. H.; Dlugogorski, B. Z. Thermal decomposition of perfluorinated carboxylic acids: Kinetic model and theoretical requirements for PFAS incineration. *Chemosphere* **2022**, *286*, 131685.
- (25) Dastgheib, S. A.; Mock, J.; Ilangoan, T.; Patterson, C. Thermogravimetric studies for the incineration of an anion exchange resin laden with short- or long-chain PFAS compounds containing carboxylic or sulfonic acid functionalities in the presence or absence of calcium oxide. *Ind. Eng. Chem. Res.* **2021**, *60* (47), 16961–16968.
- (26) Alinezhad, A.; Challa Sasi, P.; Zhang, P.; Yao, B.; Kubatova, A.; Golovko, S. A.; Golovko, M. Y.; Xiao, F. An investigation of thermal air degradation and pyrolysis of per- and polyfluoroalkyl substances and aqueous film-forming foams in soil. *ACS ES&T Eng.* **2022**, *2* (2), 198–209.
- (27) Winchell, L. J.; Ross, J. J.; Wells, M. J. M.; Fonoll, X.; Norton, J. W.; Bell, K. Y. Per- and polyfluoroalkyl substances thermal destruction at water resource recovery facilities: A state of the science review. *Water Environ. Res.* **2021**, *93* (6), 826–843.
- (28) Kundu, S.; Patel, S.; Halder, P.; Patel, T.; Hedayati Marzbali, M.; Pramanik, B. K.; Paz-Ferreiro, J.; de Figueiredo, C. C.; Bergmann, D.; Surapaneni, A.; et al. Removal of PFASs from biosolids using a semi-pilot scale pyrolysis reactor and the application of biosolids derived biochar for the removal of PFASs from contaminated water. *Environ. Sci. Water Res. Technol.* **2021**, *7*, 638–649.
- (29) Thoma, E. D.; Wright, R. S.; George, I.; Krause, M.; Preseazzi, D.; Villa, V.; Preston, W.; Deshmukh, P.; Kauppi, P.; Zemek, P. G. Pyrolysis processing of PFAS-impacted biosolids, a pilot study. *J. Air Waste Manag Assoc* **2022**, *72* (4), 309–318.
- (30) Duchesne, A. L.; Brown, J. K.; Patch, D. J.; Major, D.; Weber, K. P.; Gerhard, J. I. Remediation of PFAS-contaminated soil and granular activated carbon by smoldering combustion. *Environ. Sci. Technol.* **2020**, *54* (19), 12631–12640.
- (31) Fournie, T.; Rashwan, T. L.; Switzer, C.; Gerhard, J. I. Smouldering to treat PFAS in sewage sludge. *Waste Manage* **2023**, *164*, 219–227.
- (32) Weber, N. H.; Stockenhuber, S. P.; Delva, C. S.; Abu Fara, A.; Grimison, C. C.; Lucas, J. A.; Mackie, J. C.; Stockenhuber, M.; Kennedy, E. M. Kinetics of Decomposition of PFOS Relevant to Thermal Desorption Remediation of Soils. *Ind. Eng. Chem. Res.* **2021**, *60* (25), 9080–9087.
- (33) Crownover, E.; Oberle, D.; Kluger, M.; Heron, G. Perfluoroalkyl and polyfluoroalkyl substances thermal desorption evaluation. *Remediation* **2019**, *29* (4), 77–81.
- (34) Sörensgård, M.; Lindh, A. S.; Ahrens, L. Thermal desorption as a high removal remediation technique for soils contaminated with per- and polyfluoroalkyl substances (PFASs). *PLoS One* **2020**, *15* (6), e0234476.
- (35) Xiao, F.; Sasi, P. C.; Alinezhad, A.; Golovko, S. A.; Golovko, M. Y.; Spoto, A. Thermal decomposition of anionic, awitterionic, and cationic polyfluoroalkyl substances in aqueous film-forming foams. *Environ. Sci. Technol.* **2021**, *55* (14), 9885–9894.
- (36) Yao, B.; Sun, R.; Alinezhad, A.; Kubatova, A.; Simcik, M. F.; Guan, X.; Xiao, F. The first quantitative investigation of compounds generated from PFAS, PFAS-containing aqueous film-forming foams and commercial fluorosurfactants in pyrolytic processes. *J. Hazard Mater.* **2022**, *436*, 129313.
- (37) Shields, E. P.; Krug, J. D.; Roberson, W. R.; Jackson, S. R.; Smeltz, M. G.; Allen, M. R.; Burnette, R. P.; Nash, J. T.; Virtaranta, L.; Preston, W.; et al. Pilot-Scale Thermal Destruction of Per- and Polyfluoroalkyl Substances in a Legacy Aqueous Film Forming Foam. *ACS EST Engg.* **2023**, *3* (9), 1308–1317.
- (38) Krusic, P. J.; Roe, D. C. Gas-phase NMR technique for studying the thermolysis of materials: Thermal decomposition of ammonium perfluoroctanoate. *Anal. Chem.* **2004**, *76* (13), 3800–3803.
- (39) Hughey, K. D.; Gallagher, N. B.; Zhao, Y.; Thakur, N.; Bradley, A. M.; Koster van Groos, P. G.; Johnson, T. J. PFAS remediation: Evaluating the infrared spectra of complex gaseous mixtures to determine the efficacy of thermal decomposition of PFAS. *Chemosphere* **2024**, *362*, 142631.
- (40) Weber, N. H.; Redfern, H.; Grimison, C. C.; Lucas, J. A.; Mackie, J. C.; Stockenhuber, M.; Kennedy, E. M. Formation of Products of Incomplete Destruction (PID) from the Thermal Oxidative Decomposition of Perfluoroctanoic Acid (PFOA): Measurement, Modeling, and Reaction Pathways. *J. Phys. Chem. A* **2024**, *128*, 5362–5373.

- (41) Wang, J.; Song, M.; Abusallout, I.; Hanigan, D. Thermal Decomposition of Two Gaseous Perfluorocarboxylic Acids: Products and Mechanisms. *Environ. Sci. Technol.* **2023**, *57* (15), 6179–6187.
- (42) Sasi, P. C.; Alinezhad, A.; Yao, B.; Kubátová, A.; Golovko, S. A.; Golovko, M. Y.; Xiao, F. Effect of granular activated carbon and other porous materials on thermal decomposition of per- and polyfluoroalkyl substances: Mechanisms and implications for water purification. *Water Res.* **2021**, *200*, 117271.
- (43) Shields, E. P.; Krug, J. D.; Roberson, W. R.; Jackson, S. R.; Smeltz, M. G.; Allen, M. R.; Burnette, R. P.; Nash, J. T.; Virtaranta, L.; Preston, W.; et al. Pilot-Scale Thermal Destruction of Per- and Polyfluoroalkyl Substances in a Legacy Aqueous Film Forming Foam. *Acs Es&T Engineering* **2023**, *3* (9), 1308–1317.
- (44) Houtz, E. F.; Higgins, C. P.; Field, J. A.; Sedlak, D. L. Persistence of perfluoroalkyl acid precursors in AFFF-impacted groundwater and soil. *Environ. Sci. Technol.* **2013**, *47* (15), 8187–8195.
- (45) Wolf, N.; Mueller, L.; Enge, S.; Ungethuem, T.; Simat, T. J. Analysis of PFAS and further VOC from fluoropolymer-coated cookware by thermal desorption-gas chromatography-mass spectrometry (TD-GC-MS). *Food Addit Contam A* **2024**, *41*, 1663.
- (46) Wolf, N.; Müller, L.; Enge, S.; Ungethuem, T.; Simat, T. J. Thermal desorption - gas chromatography - mass spectrometry (TD-GC-MS) analysis of PFAS used in food contact materials. *Food Addit Contam A* **2024**, *41* (9), 1099–1117.
- (47) Yao, B.; Sun, R. Z.; Alinezhad, A.; Kubátová, A.; Simcik, M. F.; Guan, X. H.; Xiao, F. The first quantitative investigation of compounds generated from PFAS, PFAS-containing aqueous film-forming foams and commercial fluorosurfactants in pyrolytic processes. *J. Hazard. Mater.* **2022**, *436*, 129313.
- (48) Wang, J. L.; Song, M. R.; Abusallout, I.; Hanigan, D. Thermal Decomposition of Two Gaseous Perfluorocarboxylic Acids: Products and Mechanisms. *Environ. Sci. Technol.* **2023**, *57* (15), 6179–6187.
- (49) Weber, N. H.; Redfern, H.; Grimison, C. C.; Lucas, J. A.; Mackie, J. C.; Stockenhuber, M.; Kennedy, E. M. Formation of Products of Incomplete Destruction (PID) from the Thermal Oxidative Decomposition of Perfluoroctanoic Acid (PFOA): Measurement, Modeling, and Reaction Pathways. *J. Phys. Chem. A* **2024**, *128*, 5362.
- (50) Weber, N. H.; Delva, C. S.; Stockenhuber, S. P.; Grimison, C. C.; Lucas, J. A.; Mackie, J. C.; Stockenhuber, M.; Kennedy, E. M. Modeling and Experimental Study on the Thermal Decomposition of Perfluoroctanesulfonic Acid (PFOS) in an alpha-Alumina Reactor. *Ind. Eng. Chem. Res.* **2022**, *61* (16), 5453–5463.
- (51) Weber, N. H.; Dixon, L. J.; Stockenhuber, S. P.; Grimison, C. C.; Lucas, J. A.; Mackie, J. C.; Stockenhuber, M.; Kennedy, E. M. Thermal decomposition of PFOA: Influence of reactor and reaction conditions on product formation. *Chem. Eng. Sci.* **2023**, *278*, 118924.
- (52) Sun, R.; Alinezhad, A.; Altarawneh, M.; Ateia, M.; Blotevogel, J.; Mai, J.; Naidu, R.; Pignatello, J.; Rappe, A.; Zhang, X.; et al. New Insights into Thermal Degradation Products of Long-Chain Per- and Polyfluoroalkyl Substances (PFAS) and Their Mineralization Enhancement Using Additives. *Environ. Sci. Technol.* **2024**, *58* (50), 22417–22430.
- (53) Noda, I. Two-dimensional infrared spectroscopy. *J. Am. Chem. Soc.* **1989**, *111* (21), 8116–8118.
- (54) Noda, I. Chapter 2 - Advances in Two-Dimensional Correlation Spectroscopy (2DCOS). In *Frontiers and Advances in Molecular Spectroscopy*; Laane, J., Ed.; Elsevier, 2018; pp 47–75.
- (55) Czarnecki, M. A.; Morita, S. Two-Dimensional Correlation Spectroscopy. In *Near-Infrared Spectroscopy: Theory, Spectral Analysis, Instrumentation, and Applications*; Ozaki, Y., Huck, C., Tsuchikawa, S., Engelsen, S. B., Eds.; Springer Singapore, 2021; pp 111–126.
- (56) Morita, S. Chemometrics and Related Fields in Python. *Anal. Sci.* **2020**, *36* (1), 107–112.
- (57) Tanaka, M.; Hayashi, T.; Morita, S. The roles of water molecules at the biointerface of medical polymers. *Polym. J.* **2013**, *45* (7), 701–710.
- (58) Morita, S.; Shinzawa, H.; Noda, I.; Ozaki, Y. Perturbation-Correlation Moving-Window Two-Dimensional Correlation Spectroscopy. *Appl. Spectrosc.* **2006**, *60* (4), 398–406.
- (59) Vassiliadou, I.; Costopoulou, D.; Ferderigou, A.; Leondiadis, L. Levels of perfluoroctanesulfonate (PFOS) and perfluoroctanoate (PFOA) in blood samples from different groups of adults living in Greece. *Chemosphere* **2010**, *80* (10), 1199–1206.
- (60) de Haseth, J. A. Molecular Vibrations Are Not Asymmetric. *Appl. Spectrosc.* **2022**, *76* (1), 150–152.
- (61) Baker, T. J.; Tonkyn, R. G.; Thompson, C. J.; Dunlap, M. K.; Koster van Groos, P. G.; Thakur, N. A.; Wilhelm, M. J.; Myers, T. L.; Johnson, T. J. An infrared spectral database for gas-phase quantitation of volatile per- and polyfluoroalkyl substances (PFAS). *Journal of Quantitative Spectroscopy and Radiative Transfer* **2023**, *295*, 108420.
- (62) Jenness, G. R.; Shukla, M. K. What can Blyholder teach us about PFAS degradation on metal surfaces? *Environmental Science: Advances* **2024**, *3* (3), 383–401.
- (63) Lambrakos, S. G.; Shabaev, A.; Wallace, S.; Massa, L. IR Absorption Spectra for PFAS Molecules Calculated Using Density Functional Theory. Naval Research Laboratory Memorandum Report; 2020.
- (64) Wallace, S.; Lambrakos, S.; Shabaev, A.; Massa, L. Calculated IR absorption spectra for perfluoroalkyl and polyfluoroalkyl (PFAS) molecules. *Struct. Chem.* **2021**, *32* (2), 899–907.
- (65) Weber, N. H.; Grimison, C. C.; Lucas, J. A.; Mackie, J. C.; Stockenhuber, M.; Kennedy, E. M. Influence of reactor composition on the thermal decomposition of perfluoroctanesulfonic acid (PFOS). *Journal of Hazardous Materials* **2024**, *461*, 132665.
- (66) McQuarrie, D. A.; Simon, J. D. *Physical Chemistry: A Molecular Approach*; University Science Books: Sausalito, CA, 1997.
- (67) Bentel, M. J.; Yu, Y.; Xu, L.; Li, Z.; Wong, B. M.; Men, Y.; Liu, J. Defluorination of Per- and Polyfluoroalkyl Substances (PFASs) with Hydrated Electrons: Structural Dependence and Implications to PFAS Remediation and Management. *Environ. Sci. Technol.* **2019**, *53* (7), 3718–3728.
- (68) Cruz, R.; Ataka, K.; Heberle, J.; Kozuch, J. Evaluating aliphatic CF, CF₂, and CF₃ groups as vibrational Stark effect reporters. *J. Chem. Phys.* **2024**, *160* (20), 204308.
- (69) Weber, N. H.; Mackie, J. C.; Redfern, H.; Banks, E.; Grimison, C. C.; Lucas, J. A.; Stockenhuber, M.; Kennedy, E. M. Thermal mineralization of Perfluoroctanoic acid (PFOA): The synergistic role of oxygen and water vapor inhibiting products of incomplete destruction (PID) formation. *Chem. Eng. Sci.* **2025**, *301*, 120659.
- (70) Dooley, M. R.; Nixon, S. P.; Payton, B. E.; Hudak, M. A.; Odei, F.; Vyas, S. Atmospheric Oxidation of PFAS by Hydroxyl Radical: A Density Functional Theory Study. *ACS ES&T Air* **2024**, *1* (11), 1352–1361.
- (71) Pietrus, W.; Kurczab, R.; Kafel, R.; Machalska, E.; Kalinowska-Thłusick, J.; Hogendorf, A.; Żylewski, M.; Baranska, M.; Bojarski, A. J. How can fluorine directly and indirectly affect the hydrogen bonding in molecular systems? – A case study for monofluoroanilines. *Spectrochimica Acta Part A: Molecular and Biomolecular Spectroscopy* **2021**, *252*, 119536.
- (72) Xiao, F.; Challa Sasi, P.; Alinezhad, A.; Sun, R.; Abdulmalik Ali, M. Thermal Phase Transition and Rapid Degradation of Forever Chemicals (PFAS) in Spent Media Using Induction Heating. *ACS ES&T Engineering* **2023**, *3* (9), 1370–1380.
- (73) Alinezhad, A.; Shao, H.; Litvanova, K.; Sun, R.; Kubatova, A.; Zhang, W.; Li, Y.; Xiao, F. Mechanistic Investigations of Thermal Decomposition of Perfluoroalkyl Ether Carboxylic Acids and Short-Chain Perfluoroalkyl Carboxylic Acids. *Environ. Sci. Technol.* **2023**, *57* (23), 8796–8807.
- (74) Yao, B.; Sun, R.; Alinezhad, A.; Kubátová, A.; Simcik, M. F.; Guan, X.; Xiao, F. The first quantitative investigation of compounds generated from PFAS, PFAS-containing aqueous film-forming foams and commercial fluorosurfactants in pyrolytic processes. *Journal of Hazardous Materials* **2022**, *436*, 129313.
- (75) VPL Molecular Spectroscopic Database. <https://vpl.astro.washington.edu/spectra/> (accessed 2025-02-26).

- (76) Silicon tetrafluoride. NIST Chemistry WebBook, SRD 69.
<https://webbook.nist.gov/cgi/cbook.cgi?ID=C7783611&Type=IR-SPEC&Index=1#IR-SPEC> (accessed 2025-02-07).